Title

Utilisation of the Prestwick Chemical Library ® to identify drugs that inhibit the growth of Mycobacteria

Panchali Kanvatirth[a], Rose E. Jeeves[b], Joanna Bacon[b], Gurdyal S. Besra[a] and Luke J. Alderwick[a#]

[a]Institute of Microbiology and Infection, School of Biosciences, University of Birmingham, Edgbaston Park Road, Birmingham, UK, B15 2TT.

[b]Public health England, Porton down, Salisbury, UK.

[#] Address Correspondence to Luke Alderwick. Email – l.alderwick@bham.ac.uk

Tel – 0121 4145472

Running title: FDA approved drugs active against mycobacteria

Abstract

Tuberculosis (TB) is an infectious bacterial disease that kills approximately 1.3 million people every year. Despite global efforts to reduce both the incidence and mortality associated with TB, the emergence of drug resistant strains has slowed any progress made towards combating the spread of this deadly disease. The current TB drug regimen is inadequate, takes months to complete and poses significant challenges when administering to patients suffering from drug resistant TB. New treatments that are faster, simpler and more affordable are urgently required. Arguably, a good strategy to discover new drugs is to start with an old drug. Here, we have screened a library of 1200 FDA approved drugs from the Prestwick Chemical library ® using a GFP microplate assay. Drugs were screened against GFP expressing strains of *Mycobacterium smegmatis* and *Mycobacterium bovis* BCG as surrogates for *Mycobacterium tuberculosis,* the causative agent of TB in humans. We identified several classes of drugs that displayed antimycobacterial activity against both *M. smegmatis* and *M. bovis* BCG, however each organism also displayed some selectivity towards certain drug classes. Variant analysis of whole genomes sequenced for resistant mutants raised to florfenicol, vanoxerine and pentamidine highlight new pathways that could be exploited in drug repurposing programmes.

Introduction

Tuberculosis (TB) remains a major global health issue, despite it being over twenty years since the World Health Organisation (WHO) declared TB a global emergency (1). In 2016, TB killed around 1.3 million people and now ranks alongside HIV as the leading cause of death globally. It has been estimated that almost 6.3 million new cases of TB are to have occurred in 2016; 46% of these new TB cases were individuals co-infected with HIV. Alarmingly, an estimated 4.1% of new TB cases and 19% of previously treated TB cases are infections caused by Multi-Drug Resistant TB (MDR-TB), and in 2016 an estimated 190,000 people died from this form of the disease. Furthermore, extensively drug-resistant TB (XDR-TB) has now been reported in 105 countries, and accounts for approximately 30,000 TB patients in 2016. If these numbers are to reduce in line with milestones set by the WHO End TB Strategy, alternative therapeutic agents that target novel pathways are urgently required.

Drug repurposing (or drug redeployment), is an attractive approach for the rapid discovery and, in particular, development of new anti-TB drugs (2, 3). Due to the time and cost of bringing new molecular entities through the developmental pipeline to clinic, drug repurposing offers an expedient option, in part due to pre-existing pharmacological and toxicological datasets that allow for rapid profiling of active hits (4). In this study, we used GFP-expressing strains of *M. smegmatis* and *M. bovis* BCG in order to screen the Prestwick Chemical Library ® for antimycobacterial drugs. Together with drugs that have previously been identified from similar screens (5), we identified a number of novel hits that display good antimycobacterial activity which were also confirmed in

Mycobacterium tuberculosis H37Rv. We sought to characterise the mode of action of selection of hits, by performing whole genome sequencing with variant analysis on laboratory resistant mutants. This study highlights both the usefulness and circumspection required when utilising *M. smegmatis* and *M. bovis* BCG in drug repurposing screens to new anti-TB agents.

Results

Primary screening of the Prestwick Chemical Library ® against *M. smegmatis* and *M. bovis* BCG.

To identify which of the 1200 FDA approved drugs in the Prestwick Chemical Library ® inhibit the growth of mycobacteria, a high throughput fluorescence screen was used to measure GFP expression in strains of both *M. smegmatis* and *M. bovis* BCG (GFP microplate assay [GFPMA]) (6). *M. smegmatis*_pSMT3_eGFP and *M. bovis* BCG_pSMT3_eGFP were cultured in 96-well plates in the presence of 20 μM compound from the Prestwick Chemical Library ®. GFP fluorescence was measured at specified time points and data was normalized against both positive and negative controls to produce a scatter graph of the survival percentages (Fig. 1). In order to assess the reproducibility and robustness of the GFPMA HTS, we calculated Z` factor values for each of the assay plates used to screen the 1200 compounds of the Prestwick Chemical Library ® against both *M. smegmatis*_pSMT3_eGFP and *M. bovis* BCG_pSMT3_eGFP. The Z' values of the primary screen against *M. smegmatis* vary between 0.4 and 0.9 across each of the assay plates used in the screen (Fig. S1). In case of the primary screen for *M. bovis* BCG, the Z`

values are consistent between 0.8 and 0.9 across all assay plates (Fig. S1). However, since all assay plates used in the experiment derived Z' values ≥ 0.4, all data generated was deemed suitable for further processing (7). In order to understand the variability in the data and significance of the hits identified from the scatter plot (Fig. 1), we analysed the variance of data both between and across replicate experiments carried out using *M. smegmatis* and *M. bovis* BCG. The overall coefficient of correlation (r^2) values for replicate assays were calculated to be 0.63 and to 0.89 for *M. smegmatis*_pSMT3_eGFP and *M. bovis* BCG_pSMT3_eGFP, respectively (Fig. 2). This indicates increased variance in the data for assays conducted with *M. smegmatis* compared to screens performed using *M. bovis* BCG. We analysed the frequency distribution of data both within and across each primary screen using *M. smegmatis* and *M. bovis* BCG (Fig. 3). For *M. smegmatis*, we observed that 31.5 % of the compounds screened in the library induced ≤ 75 % survival of bacterial cell growth in the primary screen (Fig. 3). For BCG, 21 % of the library induced ≤ 75 % survival of bacterial cell growth in the primary screen (Fig. 3). We applied a minimum cut-off of ≤25 % bacterial cell survival at 20 μM compound, as a parameter that defined an antimycobacterial hit that would be further investigated in downstream experiments (Fig. 1). In this regard, we observed an almost identical hit rate of 6.9% and 6.8% for compounds inducing ≤ 25 % survival for *M. smegmatis* and BCG, respectively (Fig. 3).

The initial screen against *M. smegmatis* generated 83 hits which inhibited the survival of this fast-growing species of mycobacterium below 25% (Fig. 1A). The screen against the slower growing mycobacterial strain *M. bovis* BCG

123 revealed 81 hits (Fig. 1A) which inhibited the growth of the bacteria below 25%
124 (Fig. 1B). Categorisation of these hits (<25% survival) into pharmacological
125 groups reveals that an almost equal number of fluoroquinolones, macrolides,
126 polyketide antibiotics, antimycobacterial drugs, and antiseptics display
127 inhibitory activity against both *M. smegmatis* and BCG whilst the
128 aminoglycosides displayed more inhibitory activity towards *M. smegmatis*
129 compared to BCG (Fig. 4). Other notable classes of drugs that inhibit the growth
130 of both *M. smegmatis* and BCG include the amphenicols, glycopeptides and
131 non-ribosomal peptide antibiotics, antihistamines, acetylcholine esterase
132 inhibitors, antiemetic, antimalarial, antiprotozoal and surfactants (Fig. 4).
133 Notable species-specific inhibitors affecting only *M. smegmatis* were also
134 identified belonging to antiestrogen, antiarrhythmic and antipsychotic drugs (Fig.
135 4). For BCG, it appears that the cephalosporin antibiotics are only able to inhibit
136 the slower growing mycobacterial species and do not affect the faster growing
137 saprophytic organism *M. smegmatis.* Other significant drug classes that only
138 inhibit BCG include anticancer agents, antidiabetics, anticonvulsants and
139 angiotensin antagonists (Fig. 4).
140
141 All hits from the primary screen (displaying <25% survival) were filtered to
142 remove all known antimycobacterial drugs and a significant number of other
143 antimicrobial agents (5). The remaining drugs were then clustered into one of
144 three groups based upon their inhibitory activity against either fast-growing (*M.*
145 *smegmatis*) or slow-growing (*M. bovis* BCG) strains of mycobacteria, or those
146 showing overlapping activity. Each cluster of drugs was further ranked and

147 given a priority score that was based on the apparent potency of the drug and
148 potential novelty of its mode of action from literature-based searches.
149
150 **Secondary screening and hit confirmation against *M. smegmatis***
151 Minimal Inhibitory Concentrations (MIC) were determined using the
152 standardized broth dilution method and then subsequently measured on solid
153 medium in order to ascertain the concentration required to generate resistant
154 mutants (Fig. S2). Among the drugs tested against *M. smegmatis,* the most
155 potent was meclocycline sulfosalicylate with a liquid and solid MIC of 0.10 μM
156 and 0.2 μM, respectively (Table 1). Auranofin also displayed a relatively low
157 solid MIC of 6.0 μM although this was 22-fold higher than its liquid MIC values
158 (0.27 μM). Other drugs tested for MIC determination were alexidine and
159 chlorhexidine which both exhibited relatively low MIC values of 6.15μM and
160 1.98μM, both of which are used as antimicrobials in dentistry (8). The estrogen
161 receptor modulating drugs clomiphene citrate, raloxifen, toremifene and
162 tamoxifen citrate (9),(10) displayed liquid MIC values ranging from 9.03μM to
163 26.64μM (Table 1). GBR12909 (Vanoxerine), a dopamine transport inhibitor
164 (11), displayed a liquid MIC of 26.48 μM (Table 1). Two of the drugs tested
165 against *M. smegmatis*, auranofin and ebselen, displayed MIC values of 0.27μM
166 and 18.5μM respectively while other drugs which were initially identified as hits
167 from the primary screen (fendiline hydrochloride, sulocitidil, apomorphine,
168 nisoldipine, sertraline and fluspirilene) displayed relatively high MIC values that
169 ranged from 77μM to 827.5 μM (Table 1). Some drugs initially examined were
170 excluded from further solid media MIC testing (alexidine dihydrochloride,

ebselen and fluspirilene). Fluspirelene displayed a relatively high liquid MIC and alexidine dihydrochloride was discounted for further study due to its structural and functional similarity to chlorhexidine. Further investigation of ebselen ceased due to mode of action deconvolution that has been previously determined elsewhere (12). Ebselen is an organoselenium compound approved by the FDA with a well-known pharmacological profile and is currently being investigated for clinical use in the treatment of bipolar disorders and strokes. Previous studies have shown that ebselen displays antimycobacterial properties and is also effective against multidrug resistant *Staphylococcus aureus* (MRSA) (2). In *M. tuberculosis*, ebselen acts by covalently binding to an active site cysteine residue in antigen 85. Antigen 85 is a complex of secreted proteins (Ag85A, Ag85B and Ag85C) which play an important role in the synthesis of trehalose dimycolates (TDM) and mycolylarabinogalactan (mAG) (12).

Secondary screening and hit confirmation against BCG

MIC studies of the compounds listed in Table 2 revealed thonzonium bromide as having the lowest MIC value of 0.16μM. Thonzonium bromide is a quaternary ammonium monocationic compound which is used as a surfactant and a detergent and has been known to disrupt ATP dependant proton transport in vacuolar membranes along with alexidine dihydrochloride, which are responsible for pH regulation in yeast and *Candida albicans* causing growth defects (13). Florfenicol, a fluorinated analogue of thiamphenicol with broad spectrum activity against Gram negative bacteria and strains resistant to chloramphenicol and thiamphenicol (14), displayed broth and solid MIC values

of 0.67μM and 6 μM against *M. bovis* BCG, respectively (Table 2). Florfenicol is known to influence the microbiota of the intestine reducing the amount of uncultured bacterial species similar to *Corynebacterium* and *Mycobacterium* (15). Josamycin, a 16-membered macrolide with inhibitory activity against both Gram negative and Gram positive bacteria (16), displayed potent activity against BCG with an MIC of 0.1μM (Table 2). Interestingly, we identified three antihistamines as having inhibitory activity against BCG. Astemizole had the lowest MIC value of 17.8μM within this group followed by tripelennamine, with an MIC of 41.9μM and olopatadine with the highest MIC value of 202.3 μM in (Table 2). Astemizole (used for general allergies, asthma and rhinitis), tripelennamine (hay fever and rhinitis) and olopatadine (allergic conjunctivitis) are mildly anti-cholinergic and act as H1 receptor antagonists (17–20). Of the antidiabetic drugs displaying activity towards BCG, glipizide and rosiglitazone have an MIC value of 191.1 μM and 43.15 μM, respectively (Table 2). Glipizide is a second-generation sulfonylurea drug that is prescribed for hypoglycaemia in type II diabetes and is known to act by stimulating insulin production and correcting cellular lesions which occur during diabetes mellitus (21, 22). Rosiglitazone, on the other hand, functions by activating peroxisome proliferator activated receptors in adipocytes and sensitising them to insulin (23). Pinaverium, that inhibits L-type calcium channels arresting influx of the Ca^{2+} (24), had an MIC of 28.3μM. Two other drugs which displayed relatively high MIC values were granisetron and phentermine (Table 2). Granisetron, an antiemetic drug which is an agonist to the 5-hydroxytryptamine-3 receptor, stimulates the vagus nerve responsible for reflex motility response (25), had an MIC value of 210.6μM. Phentermine, which has been prescribed as an appetite

suppressant to control obesity and acts as an agonist to the human TAAR1 (Trace Amine Associate Receptor 1) (26), displayed an MIC of 375.00 μM and was not tested further due to the high concentrations required for inhibitory activity. These drugs were then further tested to establish MICs on solid media in order to determine accurate concentrations to generate spontaneous resistant mutants for mode of action studies. We observed that, upon solid agar MIC testing against BCG, the general trend was that the drugs displayed 5 to 100-fold higher MIC values when compared to MIC values obtained by broth dilution method. For some of the drugs this was attributed to low solubility in solid media as many precipitated during the cooling of the agar medium. Glipizide, olopatadine and granisetron yielded solid MIC values greater than 0.5mM; these drugs precipitated out at higher concentrations and appeared to show no noticeable inhibitory activity against BCG (Fig. S3). Rosiglitazone displayed the highest MIC value at approximately 1.5 mM. Thonzonium and florfenicol had a 5-fold increase in their solid MIC values but were still around 5μM and effectively inhibited the growth of BCG on solid agar (Table 2). Pentamidine, astemizole and pinaverium had solid MIC values of around 0.05 mM while there was a 2-fold increase in the MIC value for tripelennamine (compared to its liquid MIC) of 0.1 mM (Table 2). All compounds listed in Table 1 and Table 2 were tested in an Alamar Blur ® assay against *M. tuberculosis* (Supplementary Information) and the drugs that displayed any notable anti-TB activity are listed in Table 3. Both ebselen and auranofin displayed MICs of 18.51 μM and 0.27 μM, which are in close agreement with previously published values (12, 27). In addition, the estrogen receptor modulating drugs clomiphene and raloxifene inhibited the growth of *M. tuberculosis* H37Rv with

MICs of 7.59 μM and 22.10 μM, respectively (we were unable to accurately determine the MIC for Tamoxifen) (Table 3). Finally, GBR12909, used in the clinic to treat cocaine addiction) inhibited the growth of *M. tuberculosis* with an MIC of 26.64 μM. It is interesting to note however, that all of the drugs listed in Table 3 were identified as hits from screens conducted against *M. smegmatis* and not *M. bovis* BCG (Table 1 and Table 2).

Generation of spontaneous resistant mutants to determine mode of action.

We attempted to generate spontaneous resistant mutants in both *M. smegmatis* and BCG against a selection of drugs identified in Table 1 and Table 2, respectively. However, we were only able to obtain drug-resistant isolates for meclocyline sulfosalicylate, tamoxifen citrate and GBR12909 in *M. smegmatis* (Table 4) and florfenicol, pentamidine and tripelennamine in BCG (Table 5). Analysis of the *M. smegmatis* meclocyline sulfosalicylate mutant revealed a synonymous single nucleotide polymorphism (SNPs) mutation in the gene MSMEG_3619 (*Mtb* ortholog Rv1856c), a probable oxidoreductase deemed non-essential by the Himar-I based transposon mutagenesis [21], but also showing importance as having a growth advantage which results in an improvement in fitness when disrupted (28). A single SNP (P122S) was also observed in MSMEG_5249 (*Mtb* ortholog Rv1093) *glyA1* which is a serine hydroxymethyltransferase with possible roles of glycine to serine inter-conversion and the generation of 5, 10-methyenetetrahydrofolate which plays an important role in providing precursors for cellular redox balancing, methylation reactions and a role in thymidylate biosynthesis (Table 4). *GlyA1* is

also thought to be an essential gene (28, 29) and it has also been identified as one of the proteins which undergoes PUPylation (Ubquitinylation by prokaryotic ubiquitin protein) in mycobacteria (30). The *M. smegmatis* tamoxifen citrate resistant mutant exhibited a frame shift mutation in the gene MSMEG_6431 (*Mtb* ortholog Rv3849) *espR* which encodes for a protein involved in transcriptional regulation of the three genes Rv3136c-Rv3614c required for the ESX-1 system (Table 4). EspR binds to the promotor region and regulates ESX-1, therefore controlling virulence of mycobacteria (31). Spontaneous resistant mutants raised against GBR12909 in *M. smegmatis* produced consistent multiple mutations in MSMEG_3033 (*aroB*) (Table 4). *AroB* is predicted to be an essential gene as studied *in M. tuberculosis* (28, 29) and it encodes for 3-dehydroquinote synthase, which is one of several enzymes participating in the shikimate biosynthetic pathway (32). AroB is a homomeric enzyme, is the second enzyme in the shikimate biosynthetic pathway and is present in various bacterial species such as *Corynebacterium glutamicum*, *Escherichia coli*, *Bacillus subtilis* and other fungi, plant and apicomplexan parasites (33–35). AroB makes for an important target due to its essentiality in *M. tuberculosis* and absence of this biochemical pathway in mammals (28, 29, 33). Spontaneous resistant mutants were generated for florfenicol in BCG, revealing a point mutation in BCG_1533 (*echA12*) gene which encodes for a putative enoyl CoA hydratase (Table 5). EchA12 has been shown to be membrane localized within the mycobacterial cell membrane (36), however the gene was not found to be essential through Himar-I based transposon mutagenesis (28, 29). It has been suggested that EchA12 is involved in lipid membrane metabolism and is found to co-localise with thioredoxine A (36) and CtpD, which is an ATPase involved

296 with the metalation of proteins secreted during redox stress (37). Three
297 additional point mutations were also observed in the florfenicol resistant mutant.
298 A single guanine to adenine point mutation in the gene BCG_3185 (PPE50)
299 which encodes for a protein belonging to the PPE family, generates a G251D
300 mutation. BCG_3508 (*rpsI*) encodes for a probable 30S ribosomal protein and
301 contains a P17A mutation in the florfenicol mutant (Table 5). Florfenicol is a
302 fluorinated form of thiamphenicol which belongs to the amphenicol family of
303 antibiotics, whose mode of action is through binding to the 23S rRNA of the 50S
304 ribosomal unit (38). Finally, we also observed a V271A point mutation in
305 BCG_3755c, which encodes for a glycerol kinase (GlpK), which catalyses the
306 rate limiting step in glycerol metabolism of converting glycerol to glycerol-3-
307 phosphate (39, 40). Mutations in *glpK*, have previously been observed when
308 generating resistant mutants to drugs in an attempt to deconvolute their mode
309 of action (41, 42). In our investigation of pentamidine activity, we identified an
310 identical mutation in *glpK*, two separate non-synonymous SNPs in BCG_0763,
311 which encodes for putative membrane protein with a domain of unknown
312 function, and a single SNP in BCG_1609, which encodes for *mmpl6* (Table 5).
313 Mycobacterial membrane protein large (MmpL) are membrane proteins
314 involved in shuttling lipid components across the plasma membrane and have
315 been known to play an important role in drug resistance mechanisms,
316 membrane physiology and virulence of the bacterium (43). The tripelennamine
317 mutant had a single point mutation in the promoter region of BCG_3090, a
318 multi-drug transport integral membrane protein (*mmr*) (Table 5), which is a
319 known efflux pump involved in drug resistance with high susceptibility to
320 quaternary compounds (44). This suggest that exposure to tripelennamine

might induce a mutation that causes increased overexpression of Mmr which could alter the ability of the bacterium to efflux drugs.

Discussion

Screening compounds against *M. smegmatis* has a distinct advantage over the slower growing *M. bovis* BCG strain in terms of its shorter generation time, thus expediting the generation of screening data and turnaround of results. However, using *M. smegmatis* as a screening organism is less efficient in determining antitubercular compounds than *M. bovis* BCG. It was observed during a screen of the LOPAC library against *M. tuberculosis, M. smegmatis* and *M. bovis* BCG that 50% of the drugs inhibiting *M. tuberculosis* were not identified in *M. smegmatis* while it was only 21% of the drugs that were not identified in *M. bovis* BCG. In addition, it was observed that 30% of proteins in Mtb do not have conserved orthologs in *M. smegmatis* (5). Despite this fact, bedaquiline, the most recent drug given FDA approval for the treatment of MDR-TB, was initially discovered through a whole cell screen assay against *M. smegmatis* (45), which makes the case for not excluding *M. smegmatis* as a model organisms for antitubercular drug screening.

Although genetically similar, there are a number of physiological variations between *M. tuberculosis* and *M. bovis* BCG which have been attributed to the differential expression of around 6% of genes across their respective genomes. During the exponential growth of both organisms, major variations were observed for genes involved in cell wall processes, intermediary

metabolism and respiration and hypothetical proteins (46). In addition, in *M. tuberculosis* the PE/PPE genes were found to be highly expressed whereas in *M. bovis* BCG, there are a higher number of transcriptional regulators that are overexpressed during exponential growth. These variations in gene expression profiles of mycobacteria partly explain why different classes of drugs differentially inhibit each strain utilised during screening experiments (Fig. 4).

Target deconvolution of hits that emerge from whole cell screening efforts has long been the bottleneck of phenotypic-based drug discovery; often huge investment of time and resource is required to identify the precise molecular target of active compounds (47). Interestingly, in the case of early stage drug discovery in *M. tuberculosis*, there seems to be an apparent trend whereby inhibitors of cell growth/viability obtained through phenotypic screening efforts tend to inhibit membrane targets such as DprE1, MmpL3, QcrB and Pks13 (48). This relatively high probability of hits inhibiting membrane targets could, in part, be due to the hydrophobicity of the inhibitors screened in libraries against mycobacteria (48, 49). For instance, several drugs from the Prestwick Chemical Library ® that inhibit the growth of mycobacteria have an average clogP value of 5.7 (48). Hydrophobic drugs have a tendency to enter into the lipid layers of the mycobacterial cell envelope and then move laterally through the membrane due to their inability to cross the plasma membrane into the cytoplasm. While traversing the bilayer, these hydrophobic compounds interact with membrane proteins and thus there is an increased probability of the drugs inhibiting such targets thereby producing membrane protein related

mutations in spontaneously generated mutants during mode of action studies (48). Alexidine dihydrochloride and thonzonium bromide were amongst the hits observed in this study that have uncoupling properties and might generated a membrane protein mutation (13). In this study, screening the Prestwick Chemical Library ® also identified inhibitors such as calcium channel blockers, antihistamines, antifungal azoles and, unsurprisingly, a variety of antinfectives (Fig. 4). Calcium channel inhibitors are generally small hydrophobic molecules which have the ability to enter the phospholipid bilayer and can diffuse through the membrane inhibiting metabolic functions due to interactions with proteins and boundary lipids (50). Antifungal azoles, which have been shown to elicit inhibitory activity against mycobacteria, act by targeting the CYP121 and CYP130 cytochrome P450 systems (51). Our screening of the Prestwick Chemical Library ® and analysis of unique emerging hits, provides new impetus to explore drug repurposing as a feasible and efficient way of mining for new anti-mycobacterial drugs.

Materials and Methods

Bacterial strains, plasmids and growth media

M. smegmatis mc^2155 was electroporated with pSMT3-eGFP and transformants were selected on Tryptic Soy Agar supplemented with hygromycin B (20 µg/ml). Single colonies were used to inoculate 10 mL of Tryptic Soy Broth supplemented with Tween 80 (0.05% v/v) at 37°C with shaking at 180 rpm. *M. smegmatis* mc^2155 harbouring pSMT3-eGFP was diluted 1/100 into Middlebrook 7H9 supplemented with glycerol (2 mL/L) and Tween 80 (0.05% v/v) and further sub-cultured at 37°C with shaking at 180 rpm.

394 *M. bovis* BCG was electroporated with pSMT3-eGFP and transformants
395 selected on Middlebrook 7H10 containing OADC (10% v/v) and hygromycin B
396 (20 µg/ml). Single colonies were inoculated into 50 mL of Middlebrook 7H9
397 containing OADC (10% v/v) and Tween 80 (0.05% v/v) and statically cultured
398 at 37°C for ~ 5 days. Both *M. smegmatis* mc^2155 and *M. bovis* BCG expressing
399 eGFP were quantified by sampling 200 µL of cells which were 2-fold serially
400 diluted across a black F-bottom 96-well micro-titre plate and fluorescence was
401 measured using a BMG Labtech POLARstar Omega plate reader (Excitation
402 485-12 nm, Emission 520 nm).
403
404 **Validation of eGFP reporter screen.**
405 Batch cultures of *M. smegmatis* pSMT3-eGFP and *M. bovis* BCG pSMT3-eGFP
406 were adjusted to give a basal reading of 20,000 Relative Fluorescent Units
407 (RFU) by diluting into fresh Middlebrook 7H9 containing Tween 80 (0.05% v/v)
408 with additional OADC (10% v/v) for *M. bovis* BCG (final well volume of 200 µL).
409 The anti-mycobacterial drugs isoniazid, ethambutol, streptomycin,
410 pyrazinamide and rifampicin were included in over a range of concentrations
411 on assay plates. Wells containing mycobacterial culture in the presence of 1 %
412 DMSO represent high controls, whilst wells containing only media constitute
413 low controls. Assay plates were cultured for 48 hours in a ThermoCytomat
414 plate-shaker incubator (100 % humidity at 37°C with 180 rpm plate agitation)
415 and eGFP fluorescence was measured kinetically every 2 hours.
416
417
418

Medium Throughput Screen of the Prestwick Chemical Library ®

The Prestwick Chemical Library ® (1200 drugs) was purchased from Specs.net preformatted in master plates so that all compounds were solubilized in 100 % DMSO at a final concentration of 10 mM. A fully automated Hamilton Star work-station was used for all liquid handling protocols. Compounds were loaded into black F-bottom 96-well assay ready plates (Greiner) followed by 200 μL of either *M. smegmatis* pSMT3-eGFP or *M. bovis* BCG pSMT3-eGFP resulting in a final drug concentration of 20 μM in the primary screen. Wells containing only cells (high control) or cells in combination with 50 μg/mL rifampicin (low control) were included on each assay plate to establish positive and negative controls, respectively. Assay plates were cultured at for 48 hours in a Thermo Cytomat plate-shaker incubator (100 % humidity at 37°C with 180 rpm plate agitation) and eGFP fluorescence was measured kinetically every 2 hours to generate growth curves for individual wells of each assay plate. Data from the final 48 hr read was normalized using the following equation:

$$\%\ Survival = \left(\frac{x - \bar{x}\ (\text{negative controls})}{\bar{x}\ (\text{positive controls}) - \bar{x}\ (\text{negative controls})} \right) \times 100$$

Each assay plate was checked for robustness and reproducibility by calculating the Z'-factor using the following equation;

$$Z' = 1 - \frac{3(\sigma p + \sigma n)}{|\mu p - \mu n|}$$

For the primary screen, positive controls and negative controls were included in columns 1 and 2 respectively. The Z' was found to be on average 0.75, well above the Z'>0.5 which is widely regarded as being suitable for HTS. All 1200 drugs from the Prestwick Chemical Library ® were screened in duplicate and

443 hits were identified as inhibiting cell growth by ≥75%, as determined by
444 measuring eGFP fluorescence.
445
446 **Validation of selected hits and MIC determination in liquid media**
447 Drugs selected for further study were purchased from a variety of commercial
448 vendors. Drugs were dissolved into 100% DMSO resulting in a 10 mM stock
449 that was subsequently used to generate a 10-point 3-fold serial dilution which
450 provided a dose response curve with maximum and minimum drug
451 concentration of 500 μM and 0.0254nM, respectively. Data was normalised as
452 described above. The concentration of drug that is required to inhibit cell growth
453 by 99% was calculated by non-linear regression (Gompertz equation for MIC
454 determination, GraphPad Prism).
455
456 **MIC determination on solid agar**
457 Selected compounds identified from the secondary MIC screen were further
458 tested for MIC evaluation using solid agar media. Drugs were diluted from a
459 10mM stock, mixed individually in 2mLs of molten 7H10 agar and dispensed in
460 square partitioned petri plates. Plates were incubated at 37°C and solid MIC
461 was determined based on absence of colonies.
462
463 **Spontaneous mutant generation**
464 Spontaneous mutants were generated by plating 10^8 cells (*M. smegmatis*
465 and/or *M. bovis* BCG) per plate on 7H10 agar with drug concentrations of 2.5x,
466 5x and 10x the solid MIC values. Plates were incubated at 37 °C for a week or
467 30 days for *M. smegmatis* and *M. bovis* BCG, respectively. Colonies that

appeared on plates containing drug at 10X MIC were inoculated into 7H9 re-plated onto 7H9 agar in the presence drugs at 10X MIC in order to confirm resistance. Genomic DNA was isolated for both wild type *M. smegmatis* and *M. bovis* BCG strains together with resistant mutants (52, 53). Genomic DNA was submitted to MicrobesNG (https://microbesng.uk/) for whole genome sequencing and SNP variant analysis of the sequence in comparison to the wild type genomic DNA for each strain.

Conflicts of Interest

None to declare

Supplemental Material

Supplementary material (Figures S1 to S4) for this article are provided for online publication.

References

1. WHO | TB emergency declaration. WHO.

2. Thangamani S, Younis W, Seleem MN. 2015. Repurposing Clinical Molecule Ebselen to Combat Drug Resistant Pathogens. PLoS ONE 10:e0133877.

3. Maitra A, Bates S, Shaik M, Evangelopoulos D, Abubakar I, McHugh TD, Lipman M, Bhakta S. 2016. Repurposing drugs for treatment of tuberculosis: a role for non-steroidal anti-inflammatory drugs. Br Med Bull 118:138–148.

4. Corsello SM, Bittker JA, Liu Z, Gould J, McCarren P, Hirschman JE, Johnston SE, Vrcic A, Wong B, Khan M, Asiedu J, Narayan R, Mader CC, Subramanian A, Golub TR. 2017. The Drug Repurposing Hub: a next-generation drug library and information resource. Nat Med 23:405–408.

5. Altaf M, Miller CH, Bellows DS, O'Toole R. 2010. Evaluation of the Mycobacterium smegmatis and BCG models for the discovery of Mycobacterium tuberculosis inhibitors. Tuberculosis (Edinb) 90:333–337.

6. Collins LA, Torrero MN, Franzblau SG. 1998. Green Fluorescent Protein Reporter Microplate Assay for High-Throughput Screening of Compounds against Mycobacterium tuberculosis. Antimicrob Agents Chemother 42:344–347.

7. Zhang null, Chung null, Oldenburg null. 1999. A Simple Statistical Parameter for Use in Evaluation and Validation of High Throughput Screening Assays. J Biomol Screen 4:67–73.

8. McDonnell G, Russell AD. 1999. Antiseptics and Disinfectants: Activity, Action, and Resistance. Clin Microbiol Rev 12:147–179.

9. Boostanfar R, Jain JK, Mishell DR, Paulson RJ. 2001. A prospective randomized trial comparing clomiphene citrate with tamoxifen citrate for ovulation induction. Fertil Steril 75:1024–1026.

10. Khovidhunkit W, Shoback DM. 1999. Clinical effects of raloxifene hydrochloride in women. Ann Intern Med 130:431–439.

514 11. Andersen PH. 1989. The dopamine inhibitor GBR 12909: selectivity and
515 molecular mechanism of action. Eur J Pharmacol 166:493–504.

516 12. Favrot L, Grzegorzewicz AE, Lajiness DH, Marvin RK, Boucau J, Isailovic
517 D, Jackson M, Ronning DR. 2013. Mechanism of inhibition of
518 Mycobacterium tuberculosis antigen 85 by ebselen. Nat Commun
519 4:2748.

520 13. Chan C-Y, Prudom C, Raines SM, Charkhzarrin S, Melman SD, De Haro
521 LP, Allen C, Lee SA, Sklar LA, Parra KJ. 2012. Inhibitors of V-ATPase
522 proton transport reveal uncoupling functions of tether linking cytosolic
523 and membrane domains of V0 subunit a (Vph1p). J Biol Chem
524 287:10236–10250.

525 14. Syriopoulou VP, Harding AL, Goldmann DA, Smith AL. 1981. In vitro
526 antibacterial activity of fluorinated analogs of chloramphenicol and
527 thiamphenicol. Antimicrob Agents Chemother 19:294–297.

528 15. He S, Zhou Z, Liu Y, Cao Y, Meng K, Shi P, Yao B, Ringø E. 2010.
529 Effects of the antibiotic growth promoters flavomycin and florfenicol on
530 the autochthonous intestinal microbiota of hybrid tilapia (Oreochromis
531 niloticus ♀ × O. aureus ♂). Arch Microbiol 192:985–994.

532 16. Arsic B, Barber J, Čikoš A, Mladenovic M, Stankovic N, Novak P. 2018.
533 16-membered macrolide antibiotics: a review. Int J Antimicrob Agents
534 51:283–298.

17. Salomonsson P, Gottberg L, Heilborn H, Norrlind K, Pegelow KO. 1988. Efficacy of an oral antihistamine, astemizole, as compared to a nasal steroid spray in hay fever. Allergy 43:214–218.

18. Mah FS, O'Brien T, Kim T, Torkildsen G. 2008. Evaluation of the effects of olopatadine ophthalmic solution, 0.2% on the ocular surface of patients with allergic conjunctivitis and dry eye. Curr Med Res Opin 24:441–447.

19. Pipkorn P, Costantini C, Reynolds C, Wall M, Drake M, Sanico A, Proud D, Togias A. 2008. The effects of the nasal antihistamines olopatadine and azelastine in nasal allergen provocation. Ann Allergy Asthma Immunol 101:82–89.

20. Tardioli S, Buijs J, Gooijer C, van der Zwan G. 2012. pH-dependent complexation of histamine H1 receptor antagonists and human serum albumin studied by UV resonance Raman spectroscopy. J Phys Chem B 116:3808–3815.

21. McCaleb ML, Maloff BL, Nowak SM, Lockwood DH. 1984. Sulfonylurea effects on target tissues for insulin. Diabetes Care 7 Suppl 1:42–46.

22. Pontiroli AE, Alberetto M, Bertoletti A, Baio G, Pozza G. 1984. Sulfonylureas enhance in vivo the effectiveness of insulin in type 1 (insulin dependent) diabetes mellitus. Horm Metab Res 16 Suppl 1:167–170.

23. Hwang H-H, Moon P-G, Lee J-E, Kim J-G, Lee W, Ryu S-H, Baek M-C. 2011. Identification of the target proteins of rosiglitazone in 3T3-L1

557 adipocytes through proteomic analysis of cytosolic and secreted proteins.
558 Mol Cells 31:239–246.

559 24. Beech DJ, MacKenzie I, Bolton TB, Christen MO. 1990. Effects of
560 pinaverium on voltage-activated calcium channel currents of single
561 smooth muscle cells isolated from the longitudinal muscle of the rabbit
562 jejunum. Br J Pharmacol 99:374–378.

563 25. Navari RM, Kaplan HG, Gralla RJ, Grunberg SM, Palmer R, Fitts D.
564 1994. Efficacy and safety of granisetron, a selective 5-
565 hydroxytryptamine-3 receptor antagonist, in the prevention of nausea and
566 vomiting induced by high-dose cisplatin. J Clin Oncol 12:2204–2210.

567 26. Singh J, Kumar R. 2015. Phentermine-topiramate: First combination drug
568 for obesity. Int J Appl Basic Med Res 5:157–158.

569 27. Lin K, O'Brien KM, Trujillo C, Wang R, Wallach JB, Schnappinger D, Ehrt
570 S. 2016. Mycobacterium tuberculosis Thioredoxin Reductase Is Essential
571 for Thiol Redox Homeostasis but Plays a Minor Role in Antioxidant
572 Defense. PLOS Pathogens 12:e1005675.

573 28. DeJesus MA, Gerrick ER, Xu W, Park SW, Long JE, Boutte CC, Rubin
574 EJ, Schnappinger D, Ehrt S, Fortune SM, Sassetti CM, Ioerger TR. 2017.
575 Comprehensive Essentiality Analysis of the Mycobacterium tuberculosis
576 Genome via Saturating Transposon Mutagenesis. mBio 8:e02133-16.

577 29. Sassetti CM, Boyd DH, Rubin EJ. 2003. Genes required for
578 mycobacterial growth defined by high density mutagenesis. Mol Microbiol
579 48:77–84.

580 30. Akhter Y, Thakur S. 2017. Targets of ubiquitin like system in
581 mycobacteria and related actinobacterial species. Microbiological
582 Research 204:9–29.

583 31. Raghavan S, Manzanillo P, Chan K, Dovey C, Cox JS. 2008. Secreted
584 transcription factor controls Mycobacterium tuberculosis virulence.
585 Nature 454:717–721.

586 32. Garbe T, Servos S, Hawkins A, Dimitriadis G, Young D, Dougan G,
587 Charles I. 1991. The Mycobacterium tuberculosis shikimate pathway
588 genes: evolutionary relationship between biosynthetic and catabolic 3-
589 dehydroquinases. Mol Gen Genet 228:385–392.

590 33. Mendonça JD de, Ely F, Palma MS, Frazzon J, Basso LA, Santos DS.
591 2007. Functional Characterization by Genetic Complementation of aroB-
592 Encoded Dehydroquinate Synthase from Mycobacterium tuberculosis
593 H37Rv and Its Heterologous Expression and Purification. J Bacteriol
594 189:6246–6252.

595 34. Zhang B, Zhou N, Liu Y-M, Liu C, Lou C-B, Jiang C-Y, Liu S-J. 2015.
596 Ribosome binding site libraries and pathway modules for shikimic acid
597 synthesis with Corynebacterium glutamicum. Microb Cell Fact 14.

598 35. Lee M-Y, Hung W-P, Tsai S-H. 2017. Improvement of shikimic acid
599 production in Escherichia coli with growth phase-dependent regulation in
600 the biosynthetic pathway from glycerol. World J Microbiol Biotechnol
601 33:25.

602 36. Mawuenyega KG, Forst CV, Dobos KM, Belisle JT, Chen J, Bradbury
603 EM, Bradbury ARM, Chen X. 2005. Mycobacterium tuberculosis
604 functional network analysis by global subcellular protein profiling. Mol
605 Biol Cell 16:396–404.

606 37. Raimunda D, Long JE, Padilla-Benavides T, Sassetti CM, Argüello JM.
607 2014. Differential roles for the Co2+/Ni2+ transporting ATPases, CtpD
608 and CtpJ, in Mycobacterium tuberculosis virulence. Mol Microbiol 91.

609 38. Schifano JM, Edifor R, Sharp JD, Ouyang M, Konkimalla A, Husson RN,
610 Woychik NA. 2013. Mycobacterial toxin MazF-mt6 inhibits translation
611 through cleavage of 23S rRNA at the ribosomal A site. Proc Natl Acad
612 Sci USA 110:8501–8506.

613 39. Domenech P, Rog A, Moolji J, Radomski N, Fallow A, Leon-Solis L,
614 Bowes J, Behr MA, Reed MB. 2014. Origins of a 350-Kilobase Genomic
615 Duplication in Mycobacterium tuberculosis and Its Impact on Virulence.
616 Infect Immun 82:2902–2912.

617 40. Keating LA, Wheeler PR, Mansoor H, Inwald JK, Dale J, Hewinson RG,
618 Gordon SV. The pyruvate requirement of some members of the
619 Mycobacterium tuberculosis complex is due to an inactive pyruvate
620 kinase: implications for in vivo growth. Molecular Microbiology 56:163–
621 174.

622 41. Torrey HL, Keren I, Via LE, Lee JS, Lewis K. 2016. High Persister
623 Mutants in Mycobacterium tuberculosis. PLOS ONE 11:e0155127.

624 42. Pethe K, Sequeira PC, Agarwalla S, Rhee K, Kuhen K, Phong WY, Patel
625 V, Beer D, Walker JR, Duraiswamy J, Jiricek J, Keller TH, Chatterjee A,
626 Tan MP, Ujjini M, Rao SPS, Camacho L, Bifani P, Mak PA, Ma I, Barnes
627 SW, Chen Z, Plouffe D, Thayalan P, Ng SH, Au M, Lee BH, Tan BH,
628 Ravindran S, Nanjundappa M, Lin X, Goh A, Lakshminarayana SB,
629 Shoen C, Cynamon M, Kreiswirth B, Dartois V, Peters EC, Glynne R,
630 Brenner S, Dick T. 2010. A chemical genetic screen in Mycobacterium
631 tuberculosis identifies carbon-source-dependent growth inhibitors devoid
632 of in vivo efficacy. Nat Commun 1:57.

633 43. Viljoen A, Dubois V, Girard-Misguich F, Blaise M, Herrmann J-L, Kremer
634 L. 2017. The diverse family of MmpL transporters in mycobacteria: from
635 regulation to antimicrobial developments. Mol Microbiol 104:889–904.

636 44. Rodrigues L, Villellas C, Bailo R, Viveiros M, Aínsa JA. 2013. Role of the
637 Mmr efflux pump in drug resistance in Mycobacterium tuberculosis.
638 Antimicrob Agents Chemother 57:751–757.

639 45. Cooper CB. 2013. Development of Mycobacterium tuberculosis whole
640 cell screening hits as potential antituberculosis agents. J Med Chem
641 56:7755–7760.

642 46. Rehren G, Walters S, Fontan P, Smith I, Zárraga AM. 2007. Differential
643 gene expression between Mycobacterium bovis and Mycobacterium
644 tuberculosis. Tuberculosis (Edinb) 87:347–359.

645 47. Sharma U. 2011. Current possibilities and unresolved issues of drug
646 target validation in Mycobacterium tuberculosis. Expert Opinion on Drug
647 Discovery 6:1171–1186.

648 48. Goldman RC. 2013. Why are membrane targets discovered by
649 phenotypic screens and genome sequencing in Mycobacterium
650 tuberculosis? Tuberculosis (Edinb) 93:569–588.

651 49. Cole ST. 2016. Inhibiting Mycobacterium tuberculosis within and without.
652 Phil Trans R Soc B 371:20150506.

653 50. Catterall WA, Swanson TM. 2015. Structural Basis for Pharmacology of
654 Voltage-Gated Sodium and Calcium Channels. Mol Pharmacol 88:141–
655 150.

656 51. Ouellet H, Johnston JB, Ortiz de Montellano PR. 2010. The
657 Mycobacterium tuberculosis Cytochrome P450 System. Arch Biochem
658 Biophys 493:82–95.

659 52. Abrahams KA, Cox JAG, Spivey VL, Loman NJ, Pallen MJ,
660 Constantinidou C, Fernández R, Alemparte C, Remuiñán MJ, Barros D,
661 Ballell L, Besra GS. 2012. Identification of Novel Imidazo[1,2-a]pyridine
662 Inhibitors Targeting M. tuberculosis QcrB. PLoS One 7.

663 53. Gurcha SS, Usha V, Cox JAG, Fütterer K, Abrahams KA, Bhatt A,
664 Alderwick LJ, Reynolds RC, Loman NJ, Nataraj V, Alemparte C, Barros
665 D, Lloyd AJ, Ballell L, Hobrath JV, Besra GS. 2014. Biochemical and
666 structural characterization of mycobacterial aspartyl-tRNA synthetase
667 AspS, a promising TB drug target. PLoS ONE 9:e113568.

668 **Figure Legends**

669

670 **Fig. 1. Primary screening of the Prestwick Chemical Library ® compounds**
671 **against *M. smegmatis* (A) and *M. bovis* BCG (B) using a GFPMA assay.**
672 GFP measurements were recorded after a defined period of incubation of
673 mycobacteria in the presence of 20 μM compound from the Prestwick Chemical
674 Library ®. Data was normalised to control wells and is expressed as mean %
675 survival from n=2 biological replicate experiments. The red dashed line depicts
676 <25 % cell survival as determined by residual GFP fluorescence.

677

678 **Fig. 2. Correlation analysis of the primary screen against the** Prestwick
679 Chemical Library ®. Scatter graphs representing correlation analysis of the
680 cumulative data of the percentage survivals between n=2 biological replicate
681 experiments (run A and B) during the primary screen of the Prestwick Chemical
682 Library ® against *M. smegmatis* (A) and *M. bovis* BCG (B). The average of run
683 A and B data sets from both *M. smegmatis* (A) and *M. bovis* BCG were plotted
684 against each other (C).

685

686 **Fig. 3. A comparative frequency distribution of the primary screening**
687 **against the** Prestwick Chemical Library ®**.** Each bar represents the
688 comparative frequency distribution primary screening data (averaged) for *M.*
689 *smegmatis* (black) and *M. bovis* BCG (red). % survival data for was 'binned'
690 into groups of 5%.

691

692 **Fig. 4.** Comparison of the hits emerging from the primary screen active against
693 both *M. smegmatis* and *M. bovis* BCG. Drugs were grouped into drug
694 classifications and are plotted as frequency of hits against either *M. smegmatis*
695 or *M. bovis* BCG.
696
697

698 **FIGURE 1**

Figure 1 A

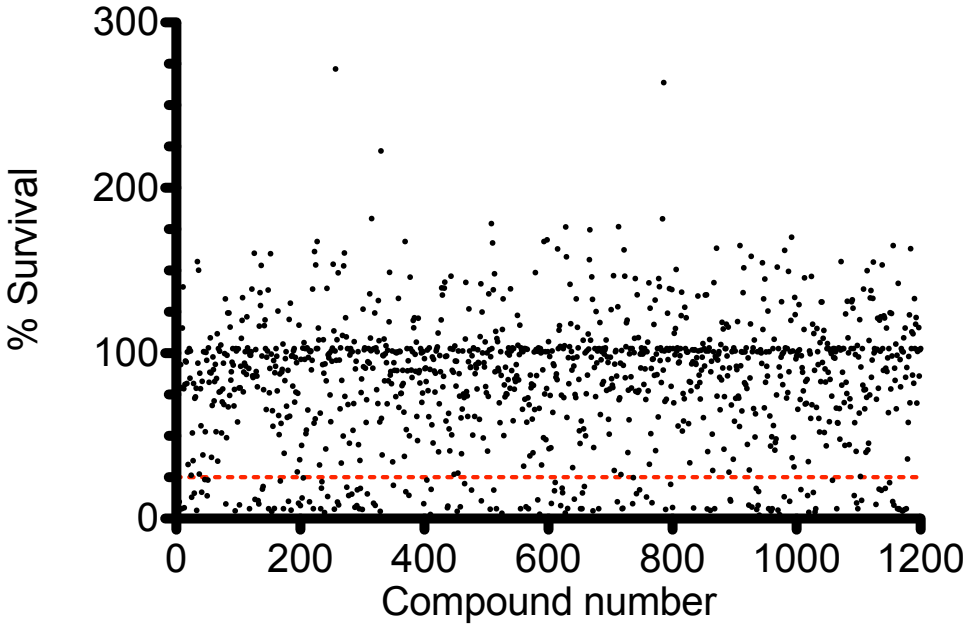

Figure 1 B

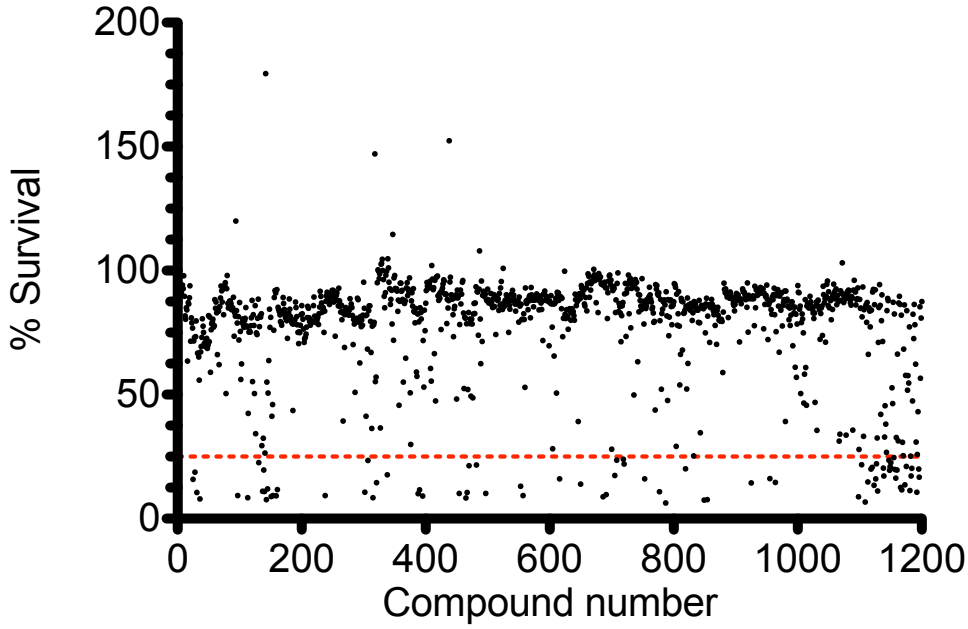

699
700

701 **FIGURE 2**

Figure 2 A

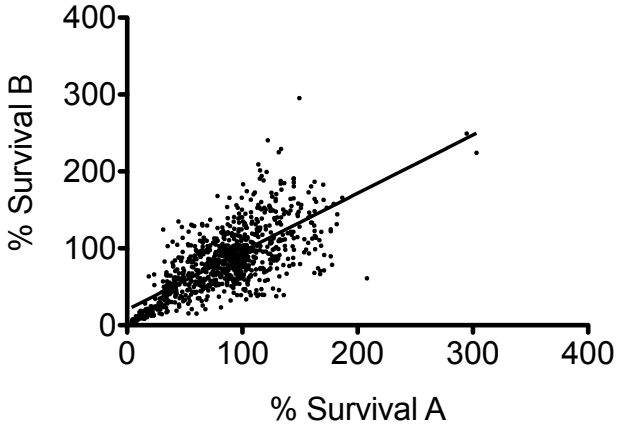

Figure 2 B

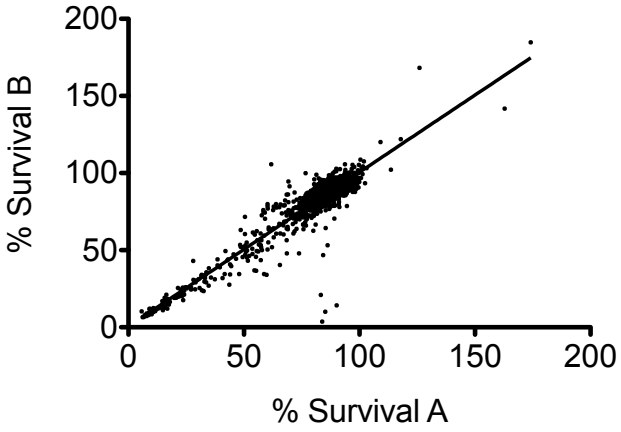

Figure 2 C

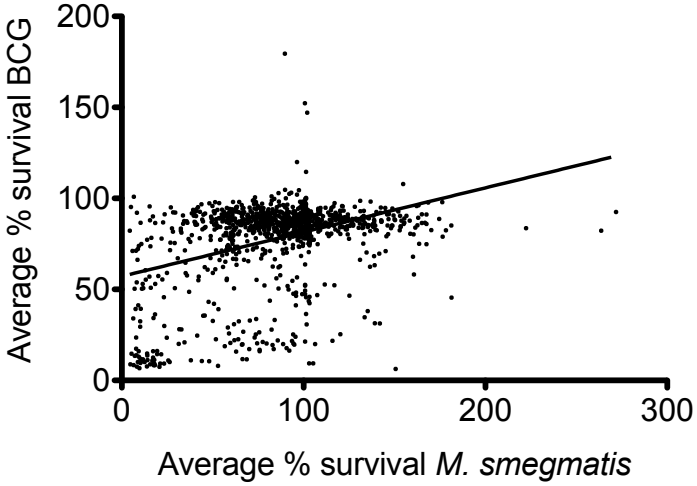

702

703 **FIGURE 3**

Figure 3

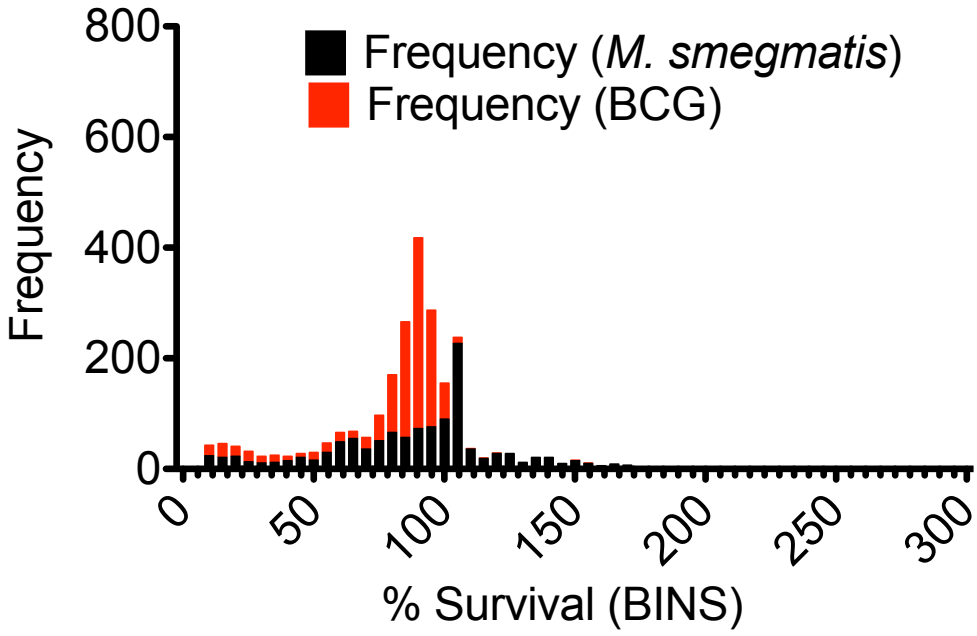

704
705

706 **FIGURE 4**

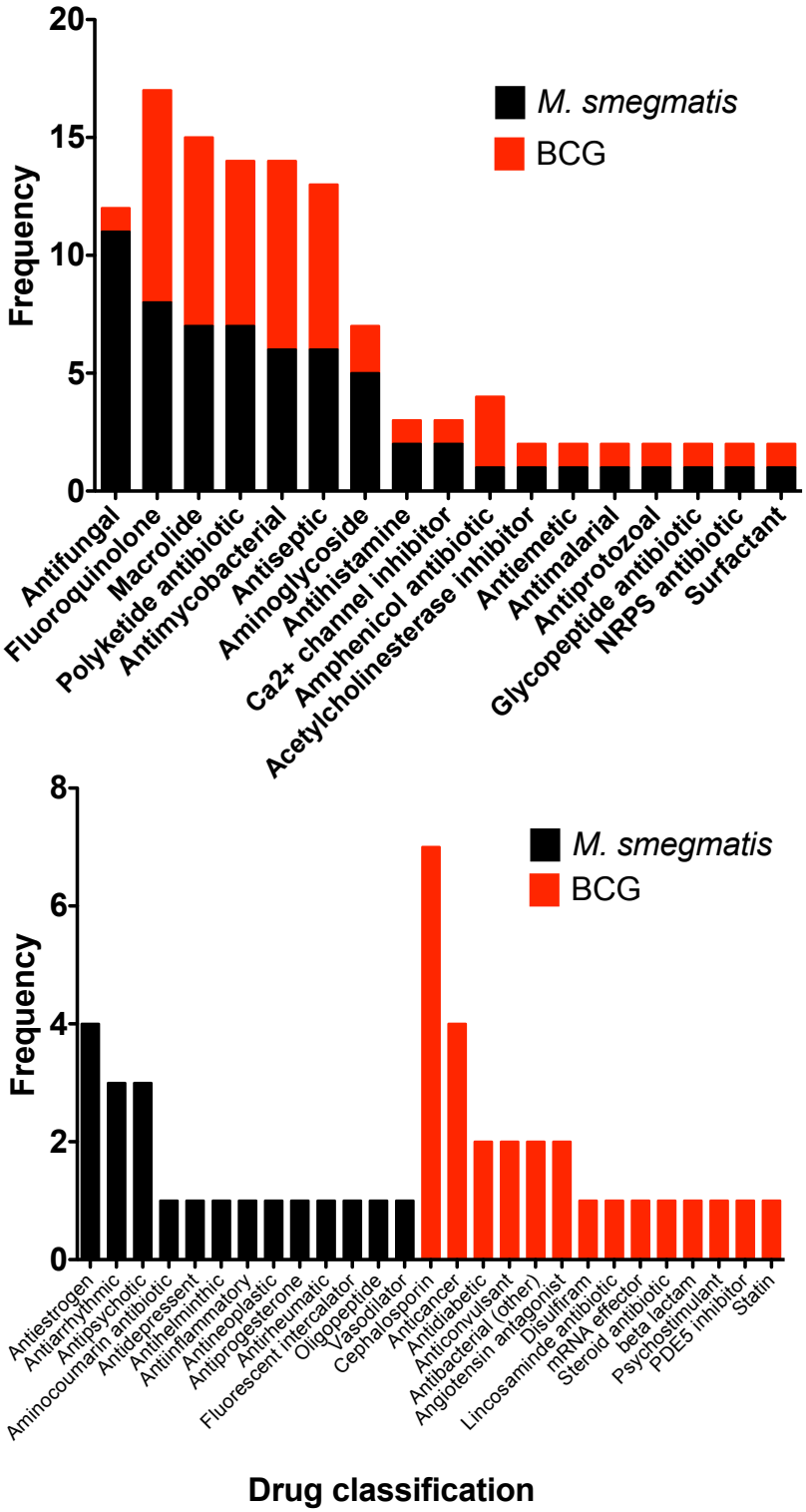

707
708
709

710

TABLES

Table 1. MIC determination of selected drugs shortlisted as hits from the whole cell screen of the Prestwick Chemical Library ® against *M. smegmatis*. MICs were determined using both liquid and solid growth mediums. (N/T) - not tested. (*) – selected for generation of drug resistant mutants.

Shortlisted Drugs (*M. smegmatis*)	**Liquid MIC (µM)**	**Solid MIC (µM)**	**Selected for generation of resistant mutants**
Meclocyline sulfosalicylate	0.10	0.20	*
Auranofin	0.27	6.0	
Chlorhexidine	1.95	16.0	
Alexidine	6.15	N/T	
Clomiphene citrate	9.03	37.5	*
Ebselen	18.51	N/T	
Raloxifene	22.1	312.5	
Toremifene	23.76	62.5	
Tamoxifen citrate	26.48	31.25	*
GBR 12909	26.64	62.5	*
Fendiline hydrochloride	77.57	15.63	
Sulocitidil	87.22	625	
Apomorphine	241.7	625	
Nisoldipine	396.2	100	
Sertraline	526.7	90	
Fluspirilene	827.5	N/T	

722 **Table 2. MIC determination of selected drugs shortlisted as hits from the**
723 **whole cell screen of the Prestwick Chemical Library ® against *M. bovis***
724 **BCG.** MICs were determined using both liquid and solid growth mediums. (N/T)
725 - not tested. (*) – selected for generation of drug resistant mutants.
726

Shortlisted Drugs (*M. bovis* BCG)	**Liquid MIC (µM)**	**Solid MIC (µM)**	**Selected generation resistant mutants**
Thonzonium	0.16	5	*
Florfenciol	0.67	6	*
Pentamidine	3.23	50	*
Astemizole	17.78	50	
Pinaverium	28.29	50	
Josamycin	0.10	100	
Tripelennamine	41.9	100	*
Rosiglitazone	43.15	≥ 1500	
Glipizide	191.10	≥ 500	
Olopatadine	202.30	≥ 500	
Granisteron	210.60	≥ 500	
Phenteramine	375.00	N/T	

727
728
729

Table 3. MIC determination of selected drugs against *M. tuberculosis* H37Rv. MICs were determined in liquid growth media using the Alamar Blue ® assay (Fig. S4).

Shortlisted Drugs (*M. tuberculosis*)	**Liquid MIC (µM)**
Ebselen	18.51
Clomiphene	7.59
GBR 12909	26.64
Raloxifen	22.10
Tamoxifen	≥ 100
Auranofin	0.27

748 **Table 4: Mode of action determination of drugs inhibiting *M. smegmatis***
749 **through whole genome sequencing and variant analysis of spontaneous**
750 **resistant mutants.** The table represents the single nucleotide polymorphisms
751 obtained through whole genome sequencing of the spontaneous resistant
752 mutants raised compared against drug sensitive *M. smegmatis*.
753
754

Drug Name (*M. smegmatis* hits)	Mutated Genes	Rv Number	Positions	Amino acid substitutions	Probable function
Meclocycline	MSMEG_3619	Rv1856c	A/G		Short chain dehydrogenase/ oxidoreductase
Meclocycline	MSMEG_5249 (*glyA1*)	Rv1093	Ccg/Tcg	P122S	Serine hydroxymethyltransferase
Tamoxifen	MSMEG_6431 (*espR*)	Rv3849	ttc/ (Frame shift)	F24	Conserved hypothetical protein
GBR12909	MSMEG_3033 (*aroB*)	Rv2538c	Ggg/Agg	G282R	Involved at the second step in the biosynthesis of chorismate within the biosynthesis of aromatic amino acids (the shikimate pathway) [catalytic activity: 7-phospho-3-deoxy-arabino-heptulosonate = 3-dehydroquinate + orthophosphate].
GBR12909	MSMEG_3033 (*aroB*)	Rv2538c	gGc/gAc	G284D	
GBR12909	MSMEG_3033 (*aroB*)	Rv2538c	Tgc.GTtgc (Frame shift)	C356V	
GBR12909	MSMEG_3033 (*aroB*)	Rv2538c	cTa/cCa	L363P	

755
756
757

Table 5: Mode of action determination of drugs inhibiting *M. bovis BCG* through whole genome sequencing and variant analysis of spontaneous resistant mutants. The table represents the single nucleotide polymorphisms obtained through whole genome sequencing of the spontaneous resistant mutants raised compared against drug sensitive *M. bovis* BCG.

Drug Name (*M. bovis* BCG hits)	Mutated Genes	Rv Number	Positions	Amino acid substitutions	Probable function
Florfenicol	BCG_1533 (EchA12)	Rv1472	Gga/Aga	G239R	Possible enoyl-CoA hydratase echA12 [*Mycobacterium bovis* BCG str. Pasteur 1173P2]
Florfenicol	BCG_3158 (PPE50)	Rv3135	gGc/gAc	G251D	PPE family protein
Florfenicol	BCG_3508 (rpsI)	Rv3442c	Ccc/Gcc	P17A	Probable 30S ribosomal protein S9 RPSI
Florfenicol	BCG_3755c (glpK)	Rv3696c	gTc/gCc	V271A	Probable glycerol kinase GlpK (ATP glycerol 3-phosphotransferase)
Pentamidine	BCG_0763	Rv0713	aTt/aCt	I274T	Probable conserved transmembrane protein [*Mycobacterium bovis* BCG str. Pasteur 1173P2]
	BCG_0763	Rv0713	gCg/gTg	A281V	Probable conserved transmembrane protein [*Mycobacterium bovis* BCG str. Pasteur 1173P2]
Pentamidine	BCG_1609 (mmpL6)	Rv1557	Gcc/Acc	A31T	Probable conserved transmembrane protein
Pentamidine	BCG_3755c (glpK)	Rv3696c	gTc/gCc	V271A	Probable glycerol kinase GlpK (ATP glycerol 3-phosphotransferase)
Trippelennamine	promoter region of gene BCG_3090	Rv3065	Upstream gene BCG 3089c (Rv 1904)		Multi-drug transport integral membrane protein (efflux pump)

	glpK	Rv3696c	gTc/gCc	V271A	Probable glycerol kinase GlpK (ATP glycerol 3-phosphotransferase)

764
765
766
767
768